Journal of Natural Sciences and Mathematics Research
J. Nat. Scien. & Math. Res. Vol. 12 No. 1 (2026) 23-40
ISSN: 2460-4453 (Online); 2614-6487 (Printed)
Available online at http://journal.walisongo.ac.id/index.php/jnsmr

Seismic activity parameters (seismicity index, annual probability, and recurrence time) estimated for the M ≥ 4.0 earthquakes in East Kolaka, Indonesia

Imanuela Indah Pertiwi[1*], Marniati[2], Joshua Purba[3], Trismahargyono[4]
[1] Kendari Geophysical Station, Indonesia Agency of Meteorology, Climatology, and Geophysics (BMKG), Indonesia
[2] Makassar Regional Center IV, Indonesia Agency of Meteorology, Climatology, and Geophysics (BMKG), Indonesia
[3] Gowa Geophysical Station, Indonesia Agency of Meteorology, Climatology, and Geophysics (BMKG), Indonesia
[4] Directorate of Earthquakes and Tsunami, Indonesia Agency of Meteorology, Climatology, and Geophysics (BMKG), Indonesia

* Corresponding author's e-mail: imanuela.pertiwi@bmkg.go.id

ABSTRACT
The M 4.9 magnitude earthquake in East Kolaka, Indonesia, that occurred on Friday, 24 January 2025, was followed by a series of other earthquakes with magnitudes ranging from M 1.2 to M 5.1. The distribution of epicenters of the earthquake series that occurred in the East Kolaka region forms a single line of convergence. Seismic activity parameters were estimated using the Maximum Likelihood method, as implemented in the ZMap 7.1 program. Using the BMKG earthquake event catalogue for the period 2021–March 2025, the a-value for the East Kolaka region—specifically at coordinates 3.9512 °S 121.685°E to 4.1625°S 121.905°E, is 4.894, indicating that annual seismic activity in that area is quite high, while the Mc value is 2.4, indicating that the frequency of earthquakes with magnitudes greater than 2.4 (M>2.4) will weaken or decrease. The seismicity index values for earthquakes with M≥4.0 are higher than those for other large-magnitude categories and decrease as magnitude increases. The probability of large-scale earthquakes in this region decreases with increasing magnitude, whether over a 1-year or a 5-year period. The M≥4.0 magnitude earthquake also has a shorter recurrence interval than other large-magnitude categories. The presence of a new active fault in the East Kolaka region, triggered by the composition of the rock strata—which consist largely of metamorphic rock—is one of the reasons for the high number of earthquakes in the area. The earthquakes that occurred in the East Kolaka region between April and October 2025 correspond to a high b-value (1.01 to 1.23), indicating that many small-magnitude earthquakes occurred and that large-magnitude earthquakes are not expected in the near future. This real-world frequency aligns perfectly with the high b-value and probability estimates derived in this study, confirming that the region is currently characterized by frequent small-scale energy releases rather than catastrophic ruptures.

Keywords:
Seismicity Index, Annual Probability, Recurrence Time, b-value, East Kolaka

Introduction

Although cataclysmic earthquakes are rare, lower-magnitude seismic events occur much more frequently (Mirwald et al., 2024). One example is the M 4.9 earthquake that struck East Kolaka on Friday (24/1) at 21:37 WITA. The event was widely felt throughout Southeast Sulawesi (East Kolaka and Kolaka III–IV MMI, Bombana III MMI). The Kendari City and North, South, and Central Konawe districts were felt with II-III MMI shaking. The quake, located 4.8 km southeast of Lalolae, caused local damage, including broken elevator glass at SMS Berjaya Kolaka Hospital.

Such an event was the first in a succession of aftershocks ranging from M 1.2 to M 5.1 that lasted for over two weeks following the initial event. The highlight of the second event took place on 29 January 2025 at 08:50 WITA. This M 5.1 earthquake was similarly located but generated stronger shaking, IV–V MMI at East Kolaka and IV MMI at Kolaka, with observations of effects reported as far as Kendari and South Konawe (III MMI).

Another characteristic is that the earthquake series in East Kolaka was caused by a combination of normal faults, indicating the existence of a newly active, uncatalogued line (Wijayanto et al., 2025). That jarring change was a shock to the scientific and public senses alike, with parts of the region long viewed as essentially low-risk due to a lack of significant seismic history. This rarity is emphasized by data from the Global Centroid-Moment-Tensor (CMT), which show that while large events were recorded near the neighboring Kolaka region in 2006 and 2011, East Kolaka remained quiet until conditions allowed such a sequence to be recorded in 2025—Lalolae-East Kolaka socio-economic impacts. As reported by the East Kolaka Regional Disaster Management Agency (BPBD) on February 13, 2025, hundreds of structures were damaged by the tremors; three homes were severely damaged, and a further 185 buildings suffered minor to moderate damage. This destruction extended beyond housing, as 3 places of worship, 5 health facilities, 9 government facilities, and 26 schools were also affected. Ultimately, the majority of the damage was localized in one district — the Lalolae Subdistrict, where essentially all activity was centered.

A robust statistical framework grounded in historical data is necessary to analyze East Kolaka's seismicity. The a and b parameters of the Gutenberg-Richter law are crucial to this research. The b-value, which measures the ratio of small to large seismic events, is especially important among these because it describes the frequency-magnitude distribution. Because it enables researchers to estimate the probability of infrequent, large-scale earthquakes by observing more frequent, lower-magnitude tremors, this parameter is a fundamental component of contemporary probabilistic seismic hazard assessments (Baker et al., 2021) and epidemic-type aftershock sequence (ETAS) prediction models (Mizrahi et al., 2024). The b-value provides profound insights into the physical condition of the crust that go beyond straightforward frequency estimates. For example, Boulanouar et al. (2025) showed that areas of high shear stress are frequently correlated with lower b-values. Mirwald et al. (2024) developed a rigorous technique to compute b-value variations that minimizes selection bias, thereby addressing potential statistical difficulties and providing a more impartial interpretation of seismic changes. Additionally, temporal variations in the b-value have proven effective in distinguishing foreshocks from mainshocks (Gulia and Wiemer, 2019), a feature that greatly improves time-dependent hazard evaluations. Significant seismic events in the past, such as the 2004 Aceh, 2008 Wenchuan, and 2011 Tohoku earthquakes, were preceded by recognizable "low b-value" signals close to their epicenters (El-Isa et al., 2014; Nanjo et al., 2012; Shi et al., 2018; Nuannin, 2005). Building on this prediction capability, Wang et al. (2021) successfully mapped possible earthquake zones for the next five years using data from 2015 to 2019.

The b-value is an important indicator for evaluating regional seismic risk, as demonstrated by many studies. A key element of this approach is the determination of homogeneous seismic zones or sources using historical geographical records (Boulanouar et al., 2025). Here, the a-value, b-value, and magnitude of completeness (Mc) are calculated by the Maximum Likelihood Method. These variables are very important for determining current seismic activity levels in East Kolaka and surrounding areas, as well as the likelihood of large earthquakes with magnitudes M≥4.0 to M≥7.0. To support the statistical results, the results are related to the specific earthquake sequence recorded between April and October 2025 and to the area's general tectonic-geological setting. This holistic approach aims to clarify the fundamental mechanisms driving large-scale seismic phenomena and their spatial distributions (Nicholas et al., 2022). Ultimately, this seismicity research serves as an important model for local mitigation efforts, guiding the construction of earthquake-resistant infrastructure and strengthening the community's preparedness for future high-intensity earthquakes.

Tectonic and Geological Conditions of East Kolaka and Surrounding Areas

Figure 1 show Sulawesi Island has a complex fault system comprising both active and inactive faults (PuSGeN, 2017). Sulawesi Island is located at the meeting point of three major tectonic plates, between the Eurasian, Australian and Philippine Sea plates, known as a triple junction. During the Early Miocene, new continental crust (the Sula Spur) was formed through collision. Subsequent Banda subduction rollback then initiated extension across the region, including Sulawesi, during the Neogene (Nugraha et al., 2022). The triple junction has resulted in complex deformation patterns on the island of Sulawesi, including both strike-slip and thrust faults. These faults are active and cause earthquakes. Faults near the subduction zone exhibit a thrust pattern, whereas land faults farther from the subduction zone exhibit a strike-slip pattern, either sinistral (left-lateral) or dextral (right-lateral). Other strike-slip faults on Sulawesi have exhibited little to no recent seismic activity, though they may be tectonically active and sources of future seismicity, based on earthquake hazard modeling and GPS studies (Cipta et al., 2016; Irsyam et al., 2020; Watkinson and Hall, 2017; Hutchings et al., 2021).

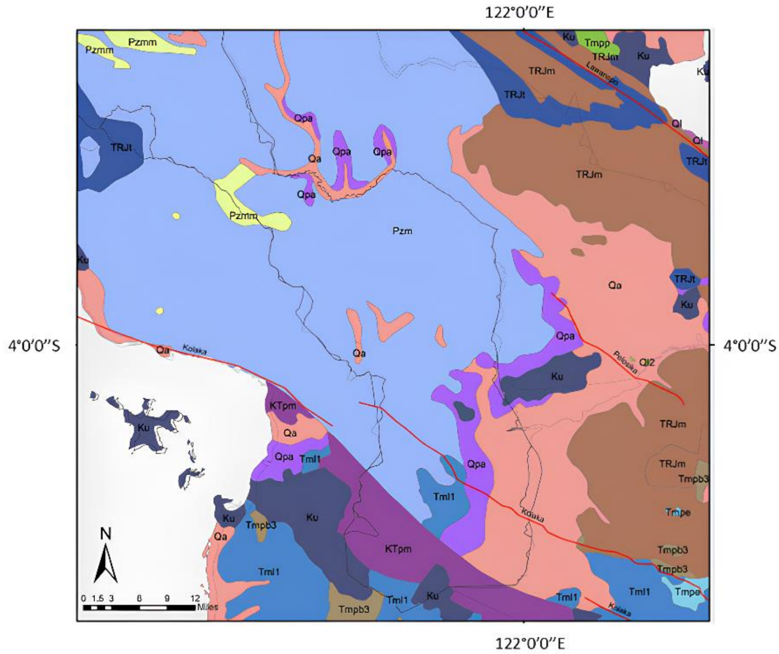

Figure 1. Geological map of East Kolaka and surrounding areas, showing red fault lines based on research results by Pusat Studi Gempa Nasional (PuSGen, 2024). Geological data from Indonesia Geospasial (2020).

Research spearheaded by the National Earthquake Study Centre (PuSGen) has reached a significant milestone with the release of the updated 2024 fault map. This latest iteration successfully identifies and delineates the Kolaka Fault system in Southeast Sulawesi, categorizing it into four distinct segments: Northern, Middle, Southern-1, and Southern-2. Additionally, the Pelosika Fault has been mapped traversing the Konawe region, which directly borders East Kolaka to the east. Characterized by strike-slip motion, these faults play a primary role in the region's seismic risk profile. Specifically, the Northern and Middle segments of the Kolaka Fault are the primary drivers of seismicity in the East Kolaka area. The Middle Kolaka Fault is of particular concern as it bisects East Kolaka, extending from the northwest in the Loea Sub-district toward the southeast in Ladongi, and continuing into the South Konawe District. Updated modeling indicates that these five fault lines possess the capacity to generate significant seismic events. The estimated maximum magnitudes (Mmax) are as follows: the Pelosika Fault at Mmax 6.6; the Northern Kolaka segment at Mmax 7.4; and the Middle Kolaka segment—most relevant to the study area—at Mmax 7.2. Furthermore, the Southern-1 and Southern-2 segments of the Kolaka Fault can generate earthquakes with Mmax values of 7.3 and 6.9, respectively (PuSGeN, 2024). Additionally, the Purpri Fault identified for the 2025 series of earthquakes in East Kolaka, defined using the HypoDD relocation method and surface deformation analysis of Sentinel-1A imagery, is also an independent seismogenic structure, not directly related to the well-known Kolaka Fault system. The fault has an oblique-normal mechanism and is the main conduit for extensional edges and left-lateral strike-slip motion; along it, only minor seismicity occurs (Purba et al., 2025).

The Southeast Arm is made up of Mesozoic sedimentary rocks, Paleogene ultrabasic and basic rocks, metamorphic rocks, and Paleogene carbonates. The metamorphic rocks in eastern Central and Southeast Sulawesi are younger (post-Eocene) than the Mesozoic metamorphic rocks in western Central Sulawesi (Mawaleda et al., 2018). The geological map in Figure 1 shows the geological structure of the research area, which is based on a combination of the Kolaka and Lasusua geological map sheets. Specifically, in the East Kolaka region, which was the main area affected by the series of earthquakes from January 29 to March 2025, the geology is dominated by medium-grade metamorphic rocks and schist (Pzm). Sedimentary, clastic, and alluvial deposits (Qa) occur in parts of northern, central, and southern East Kolaka. Sedimentary and clastic rocks with limestone (Pzmm) are distributed in the northern part, whereas the southern part contains sedimentary and clastic rocks with sandstone (Qpa). In addition, sedimentary and clastic rocks with limestone (Tml1), medium-grade metamorphic rocks and schist (KTpm), and tectonite and ophiolite rocks (Ku) are also present in the region.

Methods

The seismicity study in the East Kolaka region was based on data from earthquakes that occurred within the coordinates 3.80°S–4.34°S and 121.52°E–122.00°E. The historical earthquake event data used in the analysis includes earthquake parameters ranging from small to large magnitudes and depths less than 1000 km (h ≤ 1000 km), based on the BMKG earthquake catalogue from 2021 to March 2025. The catalog of earthquake events during that period was then processed using the Reasenberg clustering method, yielding a total of 620 events in the study area. Estimates of seismic parameters—including the seismicity index, annual probability, and recurrence time for earthquakes with M≥4 in East Kolaka—were calculated from a- and b-values using the maximum-likelihood method in Zmap 7.1, which was run via MATLAB R2024a.

Maximum Likelihood Method

The frequency-magnitude relationship of earthquakes was first introduced by Ishimoto and Iida in 1939 based on seismogram recordings for the Kwato region of Japan (Pertiwi, 2022). Then, in 1944, B. Gutenberg and C.F. Richter did the same for global data and for specific regions. In general, the frequency-magnitude relationship of earthquakes is expressed by the Gutenberg-Richter empirical equation, as shown in Equation (1).

$$Log\ (N) = a' - bM \quad (1)$$

with: $\boldsymbol{a' = a - \log\ (b \ln 10)}$

N: cumulative number of earthquakes in the study area with a magnitude greater than or equal to M.

a: regression model parameters that describe annual seismic conditions.

b: regression model parameters that describe tectonic conditions.

If the probability distribution function depending on parameters a and b is $\boldsymbol{f(M, b)}$, then the likelihood function is defined as Equation (2):

$$P\ (M, b) = f(M_1, b), f(M_2, b) \dots \dots \dots f(M_i, b) \quad (2)$$

where M_i and b are the magnitude and slope parameter (gradient) of the straight line, respectively.

If equation (2) is applied to the magnitude-frequency relationship problem, the probability distribution function $\boldsymbol{M_i}$ is given by Equation (3).

$$f(Mi, b') = b' e^{-b'(Mi - Mo)}, Mi \rangle Mo \tag{3}$$

where $\boldsymbol{b'} = \boldsymbol{b} \ln \mathbf{10}$ (Aki, 1965; Utsu, 1965). The sample likelihood function is given by Equation (4).

$$P = (b')^N \exp\left[-b'\left[\sum_{i=1}^{N} Mi - NMo\right]\right] \tag{4}$$

Based on equation (4), the estimated likelihood value of b is given by Equation (5).

$$b = \frac{log\ e}{M - Mc} \tag{5}$$

and the estimated value of a is given by Equation (6).

$$a = \log N + \log(b \ln 10) + M_c b \tag{6}$$

where N, M, and M_c are the cumulative number of data, magnitude, and magnitude completeness in the volume block under study, respectively.

A reliable seismic hazard assessment necessitates robust statistical analysis of seismic catalogs. This kind of analysis allows us to detect correlations between the physical properties of the Earth's crust and the spatio-temporal distribution of seismicity [4]. The Gutenberg-Richter (G-R) law remains the canonical approach to characterizing the frequency-magnitude relationship and provides an important framework for seismic risk evaluation and probabilistic precursor identification. The G-R relationship is expressed as: log N = a – bM, where N is the cumulative number of earthquakes with magnitude greater than M, and a and b are constants depending on the seismotectonic environment. The maximum likelihood estimation (MLE) method is commonly used to compute b-values (Mignan & Woessner, 2012; van der Elst, 2021; Lippiello and Petrillo, 2024), and the magnitude of completeness (Mc) is also determined (Chen et al., 2022) to assess statistical reliability. Interpretations of the b-parameter provide important information about the mechanical state of the crust. Low b-values have generally been associated with higher differential stress and more homogeneous rock masses, suggesting a high potential for large ruptures [e.g., 2]. On the other hand, high b-values correspond to low stress environments and high crustal heterogeneity (Zhang et al., 2025). The global average b-value is typically close to 1.0 but varies widely depending on local conditions such as thermal gradients, degree of fracturing, and shear stress concentrations (Maden and Öztürk, 2015). Thus, characterizing these variations is important for assessing the likelihood of future earthquakes and understanding the physical mechanisms controlling regional seismicity (Pertiwi, 2022; Boulanouar et al., 2025).

Seismicity Index, Annual Probability, and Recurrence Time

The seismicity index is a value that describes the total number of earthquake events that occur within a year in a research area with magnitudes greater than Mc. Seismicity index value is given by Equation (7)

$$Log\ N_1\ (M \geq M_c) = a'_1 - bM \tag{7}$$

If $\boldsymbol{a_1} = \boldsymbol{a} - \mathbf{log}\,\boldsymbol{T}$, $\boldsymbol{a'} = \boldsymbol{a_1} - \mathbf{log}(\boldsymbol{b} \ln \mathbf{10})$, and $\boldsymbol{a'_1} = \boldsymbol{a'} - \mathbf{log}\ \boldsymbol{T}$, then the equation is inverted logarithmically, so that the seismicity index equation becomes Equation (8):

$$N_1\ (M \geq M_c) = 10^{(a - \log(b \ln 10) - \log T) - bM} \tag{8}$$

where:
N ($M \geq M_c$): seismicity index for magnitude $M \geq M_c$
a dan b: constant of frequency-magnitude relationship
M: magnitude
Mc: magnitude completeness
T: time period (years of observation)

The parameters calculated as seismicity indices will provide estimates of earthquake activity in a region, enabling determination of the probability of at least one large-scale (destructive) earthquake occurring within a certain period. The probability of an earthquake with a magnitude greater than Mc occurring within a period of time T can be calculated from equation (9):

$$P\ (M \geq M_c, T\ ) = (1 - e^{-N1(M \geq Mc)\ T}) \quad (9)$$

with:
$P\ (M \geq M_c,\ T\ )$: earthquake risk level for magnitude $M \geq M_c$ with time period T
$N1\ (M \geq M_c)$: seismicity index for magnitude $M \geq M_c$
T: time period
In this study, calculations were performed to assess earthquake risk over 1-year and 5-year periods.

The recurrence time is the probability that an earthquake of a given magnitude will occur again. With the seismicity index values for each magnitude, the recurrence period of earthquakes of that magnitude can be calculated. The formula for calculating the recurrence time is as shown in Equation (10).

$$\theta\ (M) = \frac{1}{N(M \geq M_c)} \quad (10)$$

with:
θ: recurrence time (years)
M: the magnitude of the earthquake for which the recurrence time is to be calculated.
$N\ (M \geq Mc)$: seismicity index value at a given magnitude.

Zmap Program

The ZMap 7.1 software package was used to estimate the completeness magnitude (Mc) and the a and b parameters for this data set in this investigation. ZMap offers a set of automated spatial gridding techniques for seismicity analysis that aim to reduce data repetition and minimize earthquake loss, which are limitations often attributed to constant gridding methods. In contrast to conventional mapping methods, which often require manual parameter adjustments for each catalog (Godano et al., 2022), ZMap simplifies the task by generally requiring only the setting of a fixed number of events per grid node. The software enables diverse analytical outputs from this information, including spatial epicenter distributions and 2D b-value maps, as well as more general time-series analyses, such as histograms of depth, magnitude, and the daily number of events. Moreover, it enables the creation of frequency-magnitude distribution (FMD) graphs, earthquake occurrence probability curves, and estimated recurrence intervals for large earthquake events. For this analysis, Mc was estimated for each cell via the Maximum Curvature method (Wiemer and Wyss, 2000). An adjustment factor of +0.2 was applied to the initial Mc estimate, following Wiemer (2001). This downgrade creates a more conservative completeness threshold, improving the statistical reliability of the resulting b-value estimates.

The ZMap outputs give information on the multidimensional analysis of regional seismicity. Using the Frequency-Magnitude Distributions (FMD), the software calculates the a and b parameters, along with their associated uncertainties, using either the maximum-likelihood or weighted least-squares method. One may analyze these parameters as functions of depth, time, and magnitude using map views, cross-sections, or 3D models. Furthermore, ZMap facilitates the computation of local recurrence time maps and differential b-value maps to compare distinct seismic periods, as well as the generation of synthetic catalogs with constant b-values for modeling purposes (Wiemer and Wyss, 1997). A critical component of this workflow is determining the Magnitude of Completeness (Mc). This value is estimated from the deviation of the FMD from the power-law fit, ensuring that the catalog is statistically representative. ZMap allows analysis of Mc as a dynamic variable with respect to time or depth and provides spatial tools to map its distribution across the study area in both plan view and vertical cross-sections (Wiemer and Wyss, 2000).

Results and Discussions

The spatial distribution of b-values across the Kolaka and East Kolaka regions was modeled using seismic data spanning from 2021 to March 2025, with magnitudes ranging from M 1.2 to M 5.1. Using ZMap, we generated a comprehensive b-value distribution map for East Kolaka and its vicinity (Figure 2a) and the corresponding frequency-magnitude distribution (FMD) curves (Figure 2b). The calculated b-value for this region is 0.97 ± 0.05, which falls within the stable range of 0.92 to 1.02. The magnitude of completeness (Mc) was identified at M 2.1. This Mc threshold suggests that the regional catalog is dominated by small-to-moderate events, with the frequency of earthquakes exceeding M 2.1 following a characteristic power-law decay. Furthermore, temporal analysis (Figure 3) illustrates an increasing trend in b-values over the study period. This upward trajectory indicates a shift in the frequency-magnitude ratio, suggesting a currently low probability of large-scale seismic events (M≥4.0 to M≥7.0) in the immediate future.

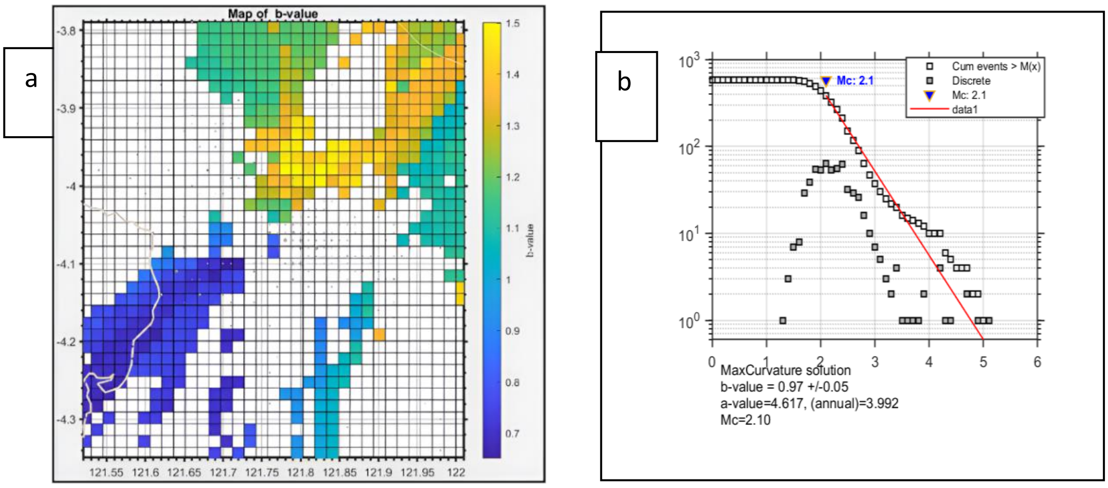

Figure 2. (a) Map of spatial variation of the seismic b-values in the East Kolaka and surrounding areas. (b) Graph of Mc (Magnitude Completeness) values, b-values and a-values in East Kolaka and surrounding areas. Plotted are both the cumulative (red line) and non-cumulative (outside the red line) forms.

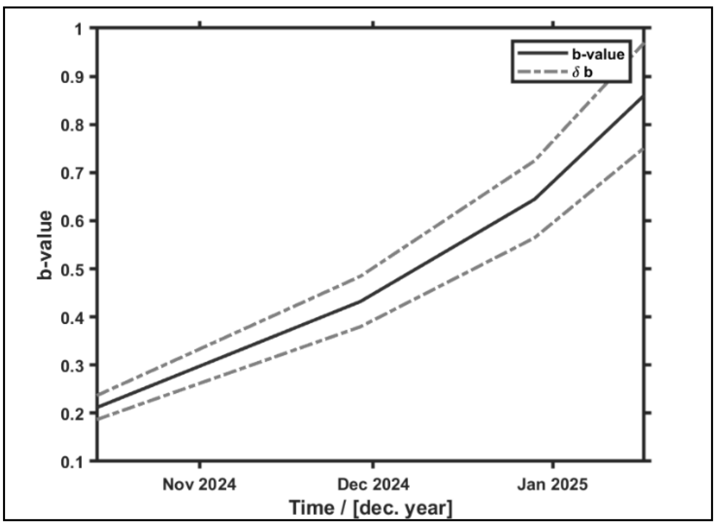

Figure 3. Graph of b-value variation over time

The epicentral distribution of the East Kolaka earthquake sequence exhibits a distinct linear alignment. To further investigate this trend, a vertical cross-section, designated as AA' (Figure 4), was constructed along the axis of these epicenters. This cross-section encompasses a rectangular domain 33.81 km long and 20 km wide, extending from 3.9512°S, 121.685°E to 4.1625°S, 121.905°E. Geographically, the AA's profile spans several administrative areas in the East Kolaka region, specifically the sub-districts of Lalolae, Mowewe, Tinondo, Uluiwoi, Ueesi, Tirawuta, Loea, Ladongi, Dangia, Polipolia, Aere, and Lambandia. This cross-sectional analysis is critical for delineating the subsurface geometry of the active fault and assessing the depth distribution of the seismic sequence relative to these local sub-districts.

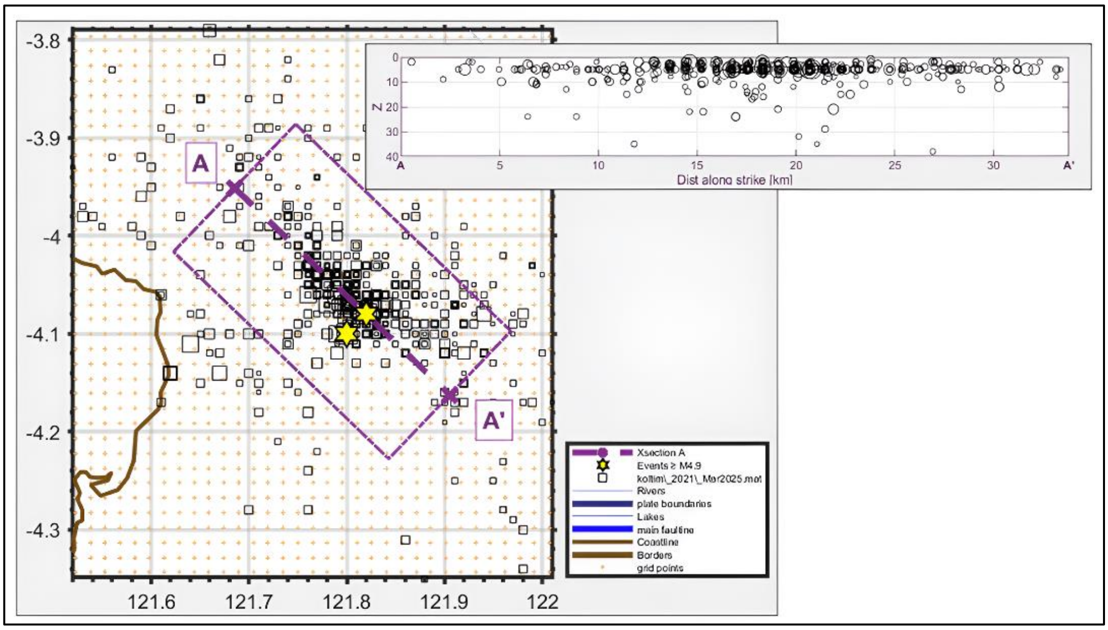

Figure 4. Cross-section of epicenter distribution in East Kolaka region (AA'). The number of earthquakes within the cross-section area totals 439, with earthquake magnitudes ranging from M 1.2 to M 5.1.

The discussion in this study focuses on the seismic evolution within the AA's cross-section of the East Kolaka region (Figure 5 and 6). From 2021 through March 2025, the area exhibited a significant rise in recorded seismic activity. In 2021, seismic events were rare; however, 2022 and 2023 saw an increase in frequency, though the temporal intervals between events remained relatively large. It is important to note that this initial uptick is likely attributable to the expansion of the regional seismic sensor network, which enhanced detection capabilities for lower-magnitude events (Pertiwi et al., 2024). By 2024, the character of the seismicity shifted toward more frequent events with shorter inter-event times (Pertiwi, 2025), though magnitudes remained predominantly below 4 (M<4.0). This intensifying trend culminated in January 2025 with the unexpected M 4.9 earthquake on January 24. This event served as the precursor to a high-magnitude cluster: a magnitude M 4.2 event occurred on January 25, followed by dual M 4.1 and M 4.2 events on January 28. The peak of this sequence occurred on January 29, 2025, with a series of significant ruptures, including M 4.7, M 4.3, and the sequence maximum of M 5.1. Through March 2025, the M 5.1 event remains the highest magnitude recorded in the East Kolaka series.

The seismic sequence in East Kolaka is characterized by persistent clusters of micro- to moderate-magnitude earthquakes (M<4.0). According to the gridded (smoothed) seismicity model proposed by Petersen et al. (2008), such clusters are instrumental in estimating future seismic event rates, as larger ruptures often occur in the vicinity of established small-to-moderate activity. This study builds upon that framework by analyzing the a-value, b-value, magnitude of completeness (Mc), and seismicity index to evaluate the probability and recurrence intervals for significant events (M≥4.0 to M≥7.0). Recent investigations confirm that the East Kolaka sequence is driven by active faulting (Wijayanto et al., 2025). Utilizing the HypoDD hypocenter relocation

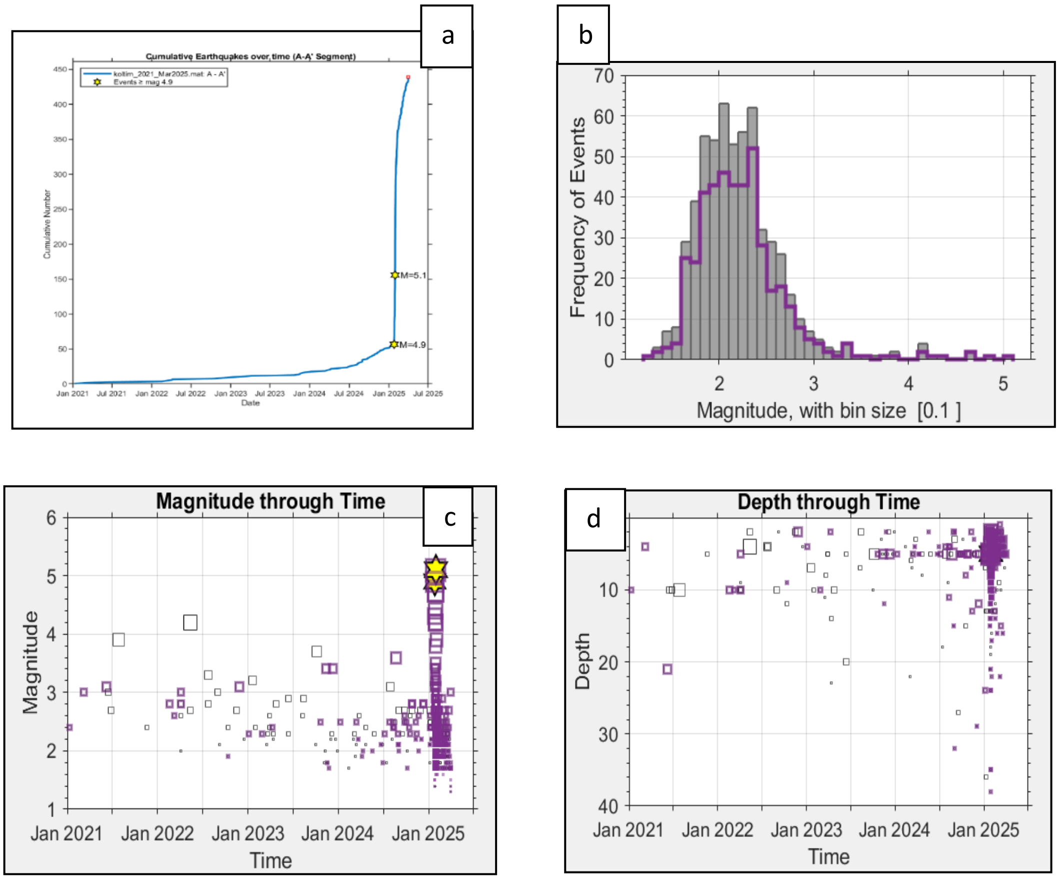

Figure 5. Cross-section time series analysis AA' (purple). (a). Cumulative frequency of earthquakes over time. (b). Histogram of earthquake frequency by magnitude. (c). Magnitude scale of earthquakes over time. (d). Distribution of earthquake depth over time

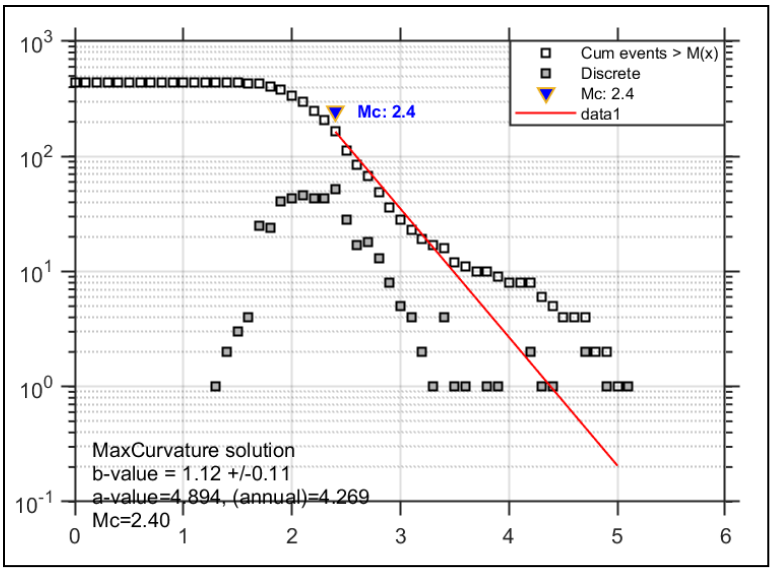

Figure 6. Frequency magnitude distribution of the overall catalogue. Plotted are both the cumulative (red line) and non-cumulative (outside the red line) forms. Also shown are the *Mc* (Magnitude Completeness), b-value and a-value in the East Kolaka region (AA'). The graph shows that the magnitude completeness (*Mc*), b-value, and a-value in the East Kolaka region are *Mc*=2.4, b-value=1.12 ± 0.11, and a-value=4.894.

method and focal mechanism analysis, researchers have determined that the source deformation is consistent with Normal Faulting. Notably, the epicentral locations of this sequence are significantly distant from the established fault systems previously mapped by the National Earthquake Study Centre in 2024. Further analysis by Purba et al. (2025) has formally identified this structure as the Purpri Fault. This identification was achieved through a multidisciplinary approach that integrated HypoDD relocation with Differential Interferometric Synthetic Aperture Radar (DInSAR). The DInSAR data provided critical evidence of land-surface deformation, specifically identifying zones of subsidence and uplift resulting from coseismic slip.

The analysis of seismic data spanning from 2021 to March 2025 indicates that b-values within the AA's cross-section of the East Kolaka range from 1.01 to 1.23 (Figure 7). In the empirical Gutenberg-Richter relationship, the a and b parameters serve as critical indicators of annual seismic productivity and regional tectonic stress regimes, respectively. Specifically, the a-value is directly proportional to the overall seismicity level, with higher values indicating a higher event frequency. The b-parameter, however, provides a window into the mechanical state of the crust. Laboratory experiments and empirical observations consistently demonstrate an inverse relationship between b-values and differential stress; as stress levels rise, b-values typically decrease (Scholz, 2015). This fundamental correlation supports the use of b-value fluctuations as a primary signal in earthquake forecasting systems (Wu et al., 2018; Spada et al., 2013; Peng et al., 2021; Ito et al., 2023; Nanjo, 2020; Beall et al., 2022). Physically, the b-value reflects the rock mass's brittleness and stress-bearing capacity. A higher b-value, as observed in this study area, suggests a more brittle or heterogeneous crust that cannot sustain high accumulated stress. Consequently, the region is characterized by frequent small-to-moderate-magnitude earthquakes, while the probability of a large-scale rupture remains significantly lower than in regions with lower b-values.

The b-values observed in the East Kolaka cross-section are notably higher than those reported in other seismically active regions across Sulawesi. For instance, significantly lower b-values have been documented in North Morowali (0.62), East Luwu (0.665) (Pertiwi, 2022), and South Buton (0.52) (Pertiwi et al., 2023). Similar low-range values, varying from 0.463 to 0.563, have also been identified in the southern portion of South Sulawesi (Pertiwi et al., 2012). In contrast, the elevated b-values within cross-section AA' indicate a highly heterogeneous crustal structure, characterized by a high frequency of small-to-medium magnitude seismic events rather than large-scale ruptures. This is further supported by an a-value of 4.894, which reflects a robust level of annual seismic productivity within the study area. Furthermore, the magnitude of completeness (Mc) was determined to be 2.4. This Mc threshold confirms that the regional seismicity is dominated by low-magnitude activity, with a predictable power-law decay in the frequency of events exceeding M>2.4.

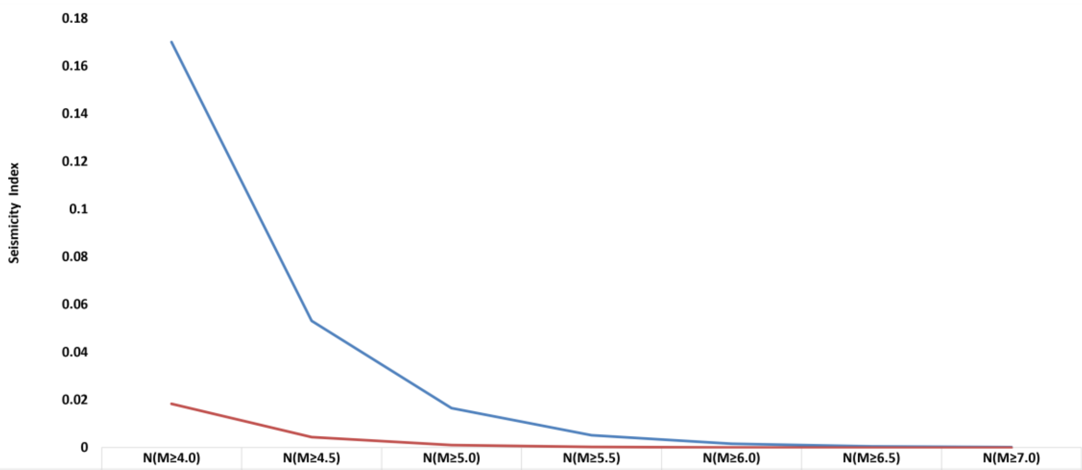

	N(M≥4.0)	N(M≥4.5)	N(M≥5.0)	N(M≥5.5)	N(M≥6.0)	N(M≥6.5)	N(M≥7.0)
b-value : 1.01	0.170092466	0.053172255	0.016622069	0.005196191	0.00162437	0.000507791	0.00015874
b-value : 1.23	0.018412016	0.004467878	0.00108418	0.000263088	6.38412E-05	1.54918E-05	3.75925E-06

Figure 7. Seismicity index values for earthquakes with M≥4.0, M≥4.5, M≥5.0, M≥5.5, M≥6, M≥6.5, and M≥7.0 in the cross-section AA' region, based on the minimum (blue line) and maximum (red line) b-values.

Recent research by Purba et al. (2025), using the scaling relationships of Wells and Coppersmith (1994), estimated that the Purpri Fault in East Kolaka extends approximately 17 km and has the potential to generate a maximum-magnitude earthquake of M 6.5. Building on this structural context, the present study calculated the seismicity index (N), annual probability, and recurrence intervals for the AA's cross-section. These parameters were evaluated for magnitude thresholds ranging from M≥4.0 to M≥7.0, accounting for both the minimum and maximum b-values observed in the region. The calculated seismicity indices, derived from Equation 6 and illustrated in Figure 7, reveal a clear spatial dependency on b-value fluctuations. Within cross-section AA', regions characterized by elevated b-values exhibit significantly lower seismicity indices for large-magnitude events. Conversely, zones with minimal b-values correlate with higher seismicity indices for larger magnitudes. These results underscore the inverse relationship between the b-value and seismic hazard: a low b-value signifies a high probability of a significant earthquake, whereas a high b-value indicates a lower probability of such events. Consistent with the Gutenberg-Richter law, the highest seismicity index values were recorded for the M≥4.0 category, with values diminishing progressively as the magnitude threshold increases. This distribution confirms that while the East Kolaka region is currently seismically active, the frequency of events decays predictably with increasing magnitude.

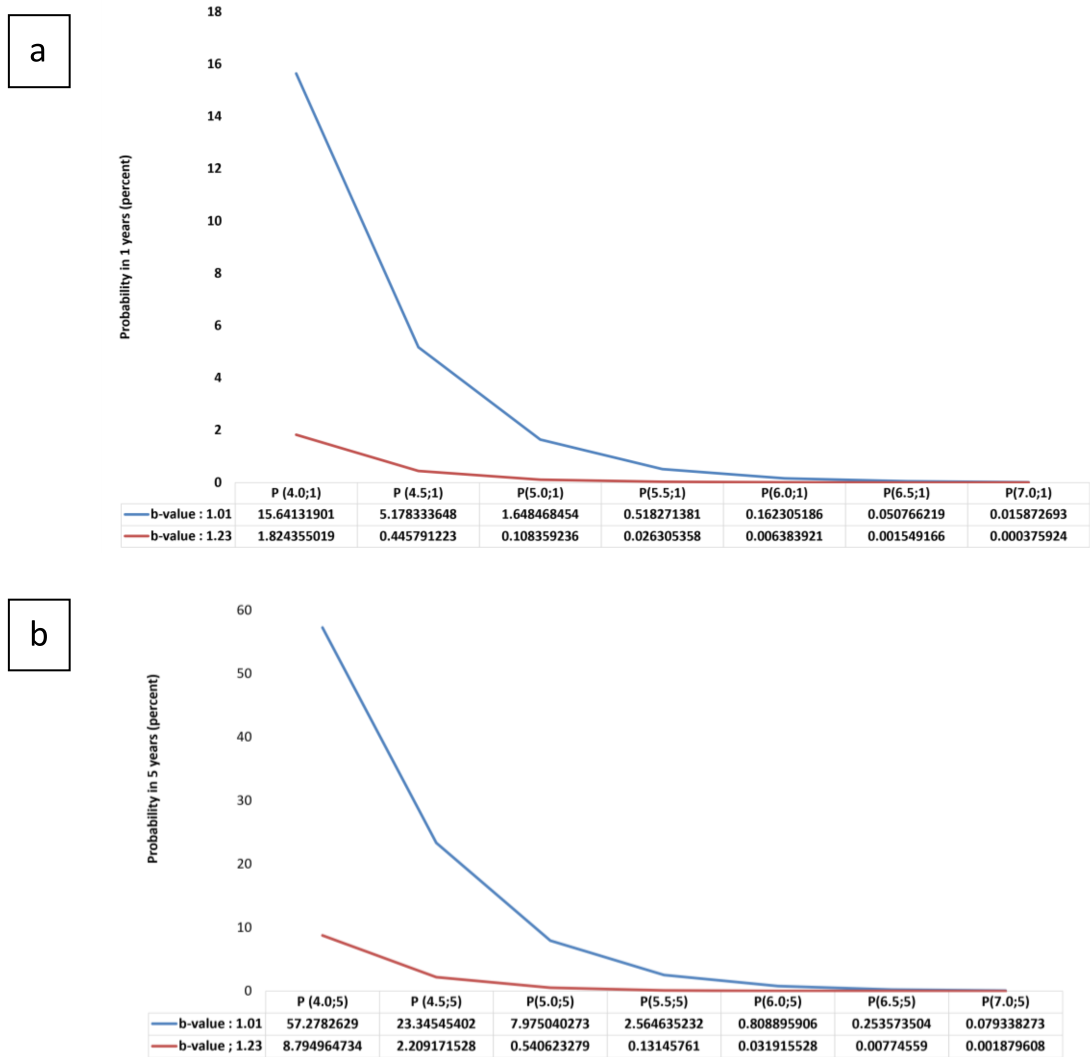

Figure 8. Annual probability of occurrence of earthquakes of magnitude M≥4.0, M≥4.5, M≥5.0, M≥5.5, M≥6, M≥6.5, and M≥7.0 in cross-section AA' based on the minimum b-value (blue line) and maximum b-value (red line), within (a) 1 year and (b) 5 years.

Utilizing the derived seismicity index, the annual probability and recurrence intervals for earthquakes within the AA's cross-section were calculated using Equations 9 and 10. The annual probability is the likelihood that at least one seismic event of a specific magnitude occurs within a defined timeframe. This analysis was conducted for magnitude thresholds from M≥4.0 to M≥7.0 over 1-year and 5-year return periods. As illustrated in Figures 8a and 8b, the b-value is inversely proportional to the annual probability of occurrence; maximum b-values correspond to lower probabilities, whereas minimum b-values indicate higher seismic risk. Based on the observed b-value range in cross-section AA', the 1-year probability (Figure 8a) for an M≥4.0 event ranges from 1.824% to 15.641%, decreasing significantly as magnitude increases (Table 1). Consistent with seismic hazard theory, the probability of a large-scale event in this region diminishes as the magnitude threshold increases across both timeframes. While the probability for any given magnitude is notably higher over 5 years than 1 year (Figure 9b), the results indicate that significant events (M≥4.0) are relatively unlikely within a single year but become increasingly probable over decadal timescales.

The recurrence time for various magnitude thresholds—ranging from M≥4.0 to M≥7.0—is illustrated in Figure 9. Our analysis demonstrates a direct correlation between magnitude and the time elapsed between events: as magnitude increases, the expected recurrence time increases significantly. A critical factor in these calculations is the local b-value. In areas with low b-values, the estimated recurrence times are notably shorter, suggesting more frequent activity. Conversely, regions with maximum b-values exhibit much longer intervals of seismic quiescence. Based on the range of b-values observed at the East Kolaka section, the estimated recurrence time range is listed in Table 1. These results indicate that earthquakes with M≥4.0 have the shortest recurrence times, with a minimum interval of just 5 years. This finding aligns closely with our previous probability analysis, which showed a high likelihood of such an event occurring within the next 5-year period.

Table 1. Probability (occurring within a 1-year and 5-year period) and recurrence time of earthquakes with magnitudes ranging from M≥4.0 to M≥7.0

Magnitude (M)	**Probability**		**Recurrence Time Range (Years)**
	1-Year probability (%)	**5-Year Probability (%)**	
M≥4.0	1.824 – 15.641	8.794 – 57.278	5 - 54
M≥4.5	0.445 – 5.178	2.209 – 23.345	18 - 223
M≥5.0	0.108 – 1.648	0.540 – 7.975	60 - 922
M≥5.5	0.026 – 0.518	0.131 – 2.564	192 – 3,801
M≥6.0	0.006 – 0.162	0.031 – 0.808	615 – 15,663
M≥6.5	0.001 – 0.050	0.007 – 0.253	1,969 – 64,550
M≥7.0	0.0003 – 0.015	0.001 – 0.079	6,299 – 266,010

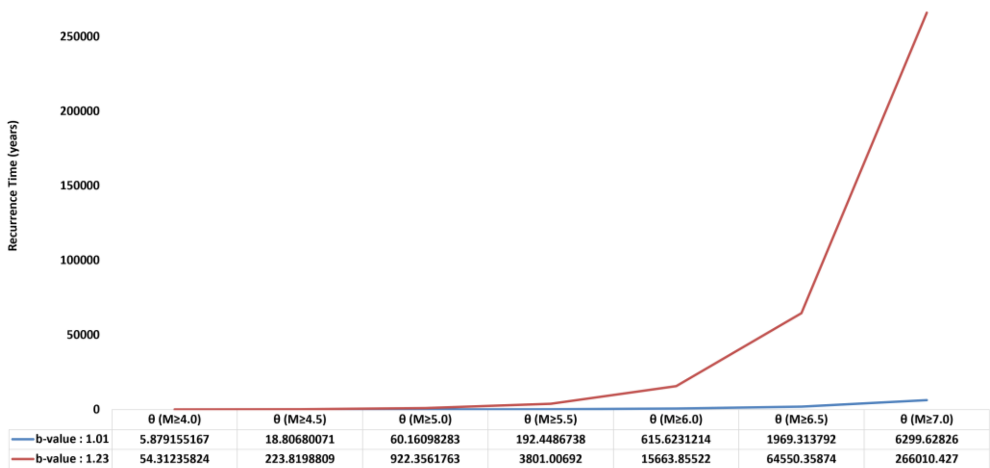

Figure 9. Recurrence time of earthquakes of magnitude M≥4.0, M≥4.5, M≥5.0, M≥5.5, M≥6, M≥6.5, and M≥7.0 in cross-section AA' based on minimum b-value (blue line) and maximum b-value (red line).

To validate the statistical results, we evaluated seismic data recorded in the BMKG earthquake parameter catalogs from April to October 2025. During this seven-month validation period, a total of 185 shallow earthquakes were recorded within the AA's cross-section of East Kolaka (Figure 10). The observed seismicity strongly aligns with our model's predictions. The vast majority of events were of low magnitude (M<4.0), with only one event exceeding this threshold: an M 4.2 earthquake in May 2025. Located 4 km southwest of Lalolae, the event reached intensities of III–IV MMI in East Kolaka and III MMI in Kolaka. Even among the smaller events (M<4.0), several were significant enough to be felt by the community, reaching intensities of II–III on the MMI scale. As defined by the USGS (https://www.usgs.gov/), the Modified Mercalli Intensity (MMI) scale measures the observed effects of an earthquake at the surface. For context, IV MMI: felt indoors by many, outdoors by few; feels like a heavy truck striking a building; III MMI: felt quite noticeably by persons indoors; vibrations similar to the passing of a truck; II MMI: felt only by a few persons at rest; delicately suspended objects may swing. The M5.1 earthquake that occurred on 29 January 2025 in Lalolae-East Kolaka reached an intensity of up to V MMI in the area, meaning that almost all local residents felt the tremors; many people woke up, and large objects swayed. This empirical validation confirms our findings that the high b-values observed in the study area accurately characterize a tectonic regime dominated by frequent, small-scale seismic releases. The absence of events exceeding M≥4.0 to M≥7.0 during this period further supports our conclusion that large-magnitude earthquakes are unlikely to occur in the immediate future within this specific cross-section.

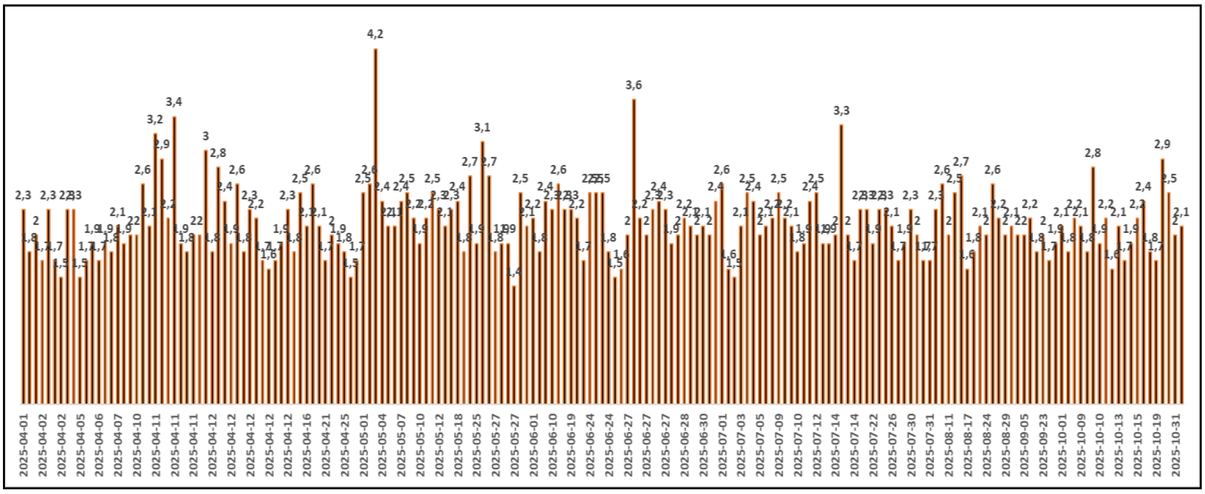

Figure 10. 185 shallow earthquake events in the AA' cross-section area of East Kolaka for the time period April to October 2025.

The total number of shallow earthquakes in the East Kolaka region over 7 months was 185 events with magnitudes less than 4 (M<4.0). This result is consistent with the earthquake activity observed from April to October 2025, according to the magnitude completeness value of Mc 2.4 obtained for AA's cross-section in East Kolaka, which indicates that earthquakes with magnitudes greater than Mc 2.4 (M>2.4) are less likely to occur. The number of earthquakes with magnitude M > 2.4 was 35, while those with magnitude less than or equal to Mc (M ≤ 2.4) were more numerous, with 150 events. The seismicity indices for M ≥ 4.0 vary between 0.018 and 0.1700, consistent with the single earthquake recorded in the following 7-month period, with magnitude M 4.2. In Fig. 7, we also observe an inverse relationship: the larger the magnitude, the smaller the seismicity index. This means that smaller magnitudes of seismic activity occur more often. During the 7-month period, 64 earthquakes had magnitudes less than 2.0 (M<2.0), 114 earthquakes had magnitudes between 2.0 and less than 3.0 (2.0≤M<3.0), and 6 earthquakes had magnitudes between 3.0 and less than 4.0 (3.0≤M<4.0).

The region's complex geological framework fundamentally drives the emergence of new active faults in East Kolaka. According to the Geological Map of Indonesia (Indonesia Geospatial, 2020), the area is primarily composed of metamorphic rocks. These rocks, formed under conditions of intense heat and pressure, possess a structural complexity far greater than that of their parent materials. This complexity manifests as intricate networks of fractures, foliation layers, and folds, which directly facilitate the development of new fault structures under tectonic stress. Beyond the earthquake source, local lithology and soil conditions significantly influence the intensity of ground shaking. While the bedrock consists of metamorphic units, the near-surface geology in the AA's cross-section area is dominated by alluvium deposits. These deposits consist of unconsolidated sand, silt, gravel, and organic matter. Furthermore, the region is characterized by extensive layers of soft clay, peat, and organic swamp soils (Geological Agency, 2019). These specific soil types are known for their high compressibility and low shear-wave velocity. Geotechnically, soft clays and fibrous peat soils act as a medium for seismic wave amplification. When earthquake waves transition from the dense metamorphic bedrock into these loose, water-saturated surface sediments, their amplitude increases. This phenomenon explains why the local community frequently reports feeling tremors even from micro-earthquakes (M<3.0). In areas with such soft soil profiles, the perceived intensity is much higher than what the earthquake magnitude alone would suggest, turning minor seismic events into noticeable local disturbances.

Statistical analyses of seismicity provide a vital framework for disaster preparedness. It is important to clarify that these models do not serve as deterministic earthquake predictions; predicting the exact timing, location, and magnitude of a future event remains a significant challenge in modern geophysics. Instead, these analyses allow us to identify seismic patterns and recurrence behaviors based on historical and current data. The insights gained from observing these patterns are indispensable for regional disaster risk management. Specifically, the high b-values and the presence of soft, liquefiable soils in the East Kolaka region necessitate a proactive approach to urban planning. Given the evidence of seismic amplification in the region's alluvium and peat deposits, local building codes must be strictly enforced. Earthquake-resistant engineering—particularly for essential public facilities—must be prioritized. Designing structures that can withstand amplified shaking in soft soil environments is the most effective way to minimize structural damage and protect the community from future seismic events.

Conclusion

Seismicity analysis of the East Kolaka region yields a magnitude of completeness (Mc) of 2.4. This indicates that the local monitoring network can detect all events above this threshold, whereas small-to-moderate events dominate the overall seismic pattern. In accordance with the Gutenberg-Richter law, the frequency of events follows a predictable power-law decay as magnitudes exceed M 2.4. The AA's cross-section exhibits b-values ranging from 1.01 to 1.23. This range is critical for assessing seismic hazard: high b-values (up to 1.23) correlate with a higher proportion of small earthquakes and a lower probability of large-scale ruptures. Low b-values (down to 1.01) indicate zones with a higher seismicity index, suggesting a relatively greater probability of larger-magnitude events.

The probability of an M≥4.0 earthquake occurring within a one-year window is estimated to range from 1.824% to 15.641%, with the likelihood decreasing sharply for higher magnitudes. While large-scale events (M≥4.0 to M≥7.0) are statistically unlikely to occur within a single year, the probability increases significantly over decadal timescales. The recurrence time for these events is notably shorter in zones with minimal b-values. For M≥4.0 events, the recurrence interval is faster than for any other large-magnitude category, aligning with the observed frequency of recent activity. The local geological setting plays a significant role in how these earthquakes are perceived. Many epicenters are located in areas characterized by alluvial deposits and soft soil structures. These conditions lead to seismic amplification, which explains why residents in nearby villages frequently feel microearthquakes (magnitudes 1.0 to 3.0). Our model was validated by seismic data from April to October 2025, which recorded over 100 shallow earthquakes. During this period, only one event exceeded the M≥4.0 threshold—an M 4.2 earthquake. This real-world frequency aligns perfectly with the high b-value and probability estimates derived in this study, confirming that the region is currently characterized by frequent small-scale energy releases rather than catastrophic ruptures.

Thus, these findings become an important scientific basis for earthquake risk mitigation and policy in East Kolaka through a strict two-pronged approach. The first is Risk-Sensitive Land-Use Planning: local authorities (e.g., BPBD and Dinas PUPR) need to immediately conduct detailed seismic microzonation mapping to identify areas with the highest amplification factors within alluvial zones. The b-value and soft-soil distribution maps should be fully integrated into the Rencana Detail Tata Ruang (RDTR) of East Kolaka to establish legal spatial control. This incorporation will legally prevent the construction of critical infrastructure (e.g., hospitals, schools, government centers, and primary evacuation routes) in low b-value/high-risk areas and rezone these lands for green open spaces, agriculture, or low-density developments. Second, structural Resiliency and Engineering: All future structural designs must strictly comply with the national seismic building codes (SNI 1726) and apply the specific structural engineering criteria mandated for Class SE (soft soil) sites, to withstand the amplified seismic waves characteristic of local alluvial formations. In addition, targeted retrofit programs and technical training for local builders are needed to improve the durability of existing residential and public buildings to increased ground motions.

Acknowledgments

The author would like to thank the Indonesian Meteorology, Climatology and Geophysics Agency (BMKG) for providing data on earthquake parameters in East Kolaka and surrounding areas.

Conflicts of interest

The authors declare that there are no conflicts of interest.

References

Aki, K. (1965). Maximum likelihood estimate of b in the formula logN = a-bM and its confidence limits. *Bulletin of the Earthquake Research Institute*, *43*, 237–239.

Badan Meteorologi, Klimatologi, dan Geofisika (BMKG). (n.d.). *Earthquake parameter catalogue*. Retrieved February 1, 2025 and November 6, 2025, from Indonesian Earthquake Catalog: Regional Event Downloader.

Baker, J., Bradley, B., & Stafford, P. (2021). *Seismic hazard and risk analysis* (1st ed.). Cambridge University Press. https://doi.org/10.1017/9781108425056

Beall, A., van den Ende, M., Ampuero, J. P., Capitanio, F. A., & Fagereng, Å. (2022). Linking earthquake magnitude-frequency statistics and stress in visco-frictional fault zone models. *Geophysical Research Letters*, *49*, Article e2022GL099247.

Boulanouar, A., Khalil, A., Sebbani, J., El Ouali, A., & Rahmouni, A. (2025). Geographic distribution of b-value in North Morocco and its surrounding for seismic zones identification. *Jordan Journal of Earth and Environmental Sciences*, *16*(1), 11–16.

Chen, X., Li, Y., & Chen, L. (2022). The characteristics of the b-value anomalies preceding the 2004 Mw9.0 Sumatra earthquake. *Geomatics, Natural Hazards and Risk*, *13*, 390–399.

Cipta, A., Robiana, R., Griffin, J. D., Horspool, N., Hidayati, S., & Cummins, P. (2016). A probabilistic seismic hazard assessment for Sulawesi, Indonesia. In P. R. Cummins & I. Meilano (Eds.), *Geohazards in Indonesia: Earth science for disaster risk reduction* (Geological Society, London, Special Publications, Vol. 441, pp. 133–152). Geological Society of London. https://doi.org/10.1144/SP441.6

El-Isa, Z. H., & Eaton, D. W. (2014). Spatiotemporal variations in the b-value of earthquake magnitude–frequency distributions: Classification and causes. *Tectonophysics*, *615–616*, 1–11.

Geological Agency. (2019). *Atlas sebaran tanah lunak Indonesia*. Kementerian Energi dan Sumber Daya Mineral.

Global Centroid-Moment-Tensor (CMT) Project. (n.d.). *Global CMT catalog search*. Retrieved February 06, 2025, from https://www.globalcmt.org/

Godano, C., Convertito, V., Pino, N. A., & Tramelli, A. (2022). An automated method for mapping independent spatial b-values. *Earth and Space Science*, *9*, Article e2021EA002205. https://doi.org/10.1029/2021EA002205

Gulia, L., & Wiemer, S. (2019). Real-time discrimination of earthquake foreshocks and aftershocks. *Nature*, *574*, 193–199. https://doi.org/10.1038/s41586-019-1606-4

Gutenberg, B., & Richter, C. F. (1944). Frequency of earthquakes in California. *Bulletin of the Seismological Society of America*, *34*(4), 185–188.

Hutchings, S. J., & Mooney, W. D. (2021). The seismicity of Indonesia and tectonic implications. *Geochemistry, Geophysics, Geosystems*, *22*, Article e2021GC009812. https://doi.org/10.1029/2021GC009812

Indonesia Geospasial. (2020). Shapefile (SHP) geologi Provinsi Sulawesi Tenggara. https://www.indonesia-geospasial.com/2020/03/download-data-shapefile-shp-geologi-se.html

Irsyam, M., Cummins, P. R., Asrurifak, M., Faizal, L., Natawidjaja, D. H., Widiyantoro, S., Meilano, I., Triyoso, W., Rudiyanto, A., Hidayati, S., Ridwan, M., Hanifa, N. R., & Syahbana, A. J. (2020). Development of the 2017 national seismic hazard maps of Indonesia. *Earthquake Spectra*, *36*(1_suppl), 112–136. https://doi.org/10.1177/8755293020951206

Ishimoto, M., & Iida, K. (1939). Observations sur les séismes enregistrés par le micro-séismographe construit dernièrement. *Bulletin of the Earthquake Research Institute*, *17*(2), 443–478.

Ito, R., & Kaneko, Y. (2023). Physical mechanism for a temporal decrease of the Gutenberg-Richter b-value prior to a large earthquake. *Journal of Geophysical Research: Solid Earth*, *128*, Article e2023JB027413.

Lippiello, E., & Petrillo, G. (2024). b-more-incomplete and b-more-positive: Insights on a robust estimator of magnitude distribution. *Journal of Geophysical Research*, *129*(2), Article e2023JB027849. https://doi.org/10.1029/2023JB027849

Maden, N., & Öztürk, S. (2015). Seismic b-values, Bouguer gravity and heat flow data beneath Eastern Anatolia, Turkey: Tectonic implications. *Surveys in Geophysics*, *36*, 549–570.

Mawaleda, M., Husain, J. R., Forster, M., Suparka, E., Abdullah, C. I., Basuki, N. I., & Hutabarat, J. (2018). Miocene tectonic of the Southeast Arm of Sulawesi, Indonesia: Based on petrology data, geochemistry, and 40Ar/39Ar geochronology of metamorphic rocks from Rumbia Complex. *IOP Conference Series: Earth and Environmental Science*, *212*, Article 012043. https://doi.org/10.1088/1755-1315/212/1/012043

Mignan, A., & Woessner, J. (2012). Estimating the magnitude of completeness for earthquake catalogs. *Community Online Resource for Statistical Seismicity Analysis*. https://doi.org/10.5078/corssa-00180805

Mirwald, A., Mizrahi, L., & Wiemer, S. (2024). How to b-significant when analyzing b-value variations. *Seismological Research Letters*. Advance online publication. https://doi.org/10.1785/0220240190

Mizrahi, L., Dallo, I., van der Elst, N. J., & Christophersen, A. (2024). Developing, testing, and communicating earthquake forecasts: Current practices and an elicitation of expert recommendations. *Reviews of Geophysics*, *62*, Article e2023RG000823. https://doi.org/10.1029/2023RG000823

Nanjo, K. Z., Hirata, N., Obara, K., & Kasahara, K. (2012). Decade-scale decrease in b value prior to the M9-class 2011 Tohoku and 2004 Sumatra quakes. *Geophysical Research Letters*, *39*, Article L20304.

Nanjo, K. Z. (2020). Were changes in stress state responsible for the 2019 Ridgecrest, California, earthquakes? *Nature Communications*, *11*, Article 3082.

Nicholas, O., Dickson, M. N., & Okeke, F. O. (2022). Building collapse in Nigeria and its consequences on the architect's role as the leader of the building team. *Jordan Journal of Earth and Environmental Sciences*, *13*(1), 16–25.

Nuannin, P. (2005). Spatial and temporal b value anomalies preceding the devastating off coast of NW Sumatra earthquake of December 26, 2004. *Geophysical Research Letters*, *32*, Article L11307.

Nugraha, A. M. S., Hall, R., & BouDagher-Fadel, M. (2022). The Celebes Molasse: A revised Neogene stratigraphy for Sulawesi, Indonesia. *Journal of Asian Earth Sciences*, *228*, 1–28.

Peng, G., Lei, X., Wang, G., & Jiang, F. (2021). Precursory tidal triggering and b value variation before the 2011 Mw 5.1 and 5.0 Tengchong, China earthquakes. *Earth and Planetary Science Letters*, *574*, Article 117167.

Pertiwi, I. I., Arsyad, M., & Palloan, P. (2012). Analisis distribusi spasial dan temporal seismotektonik wilayah Sulawesi bagian selatan dan barat berdasarkan nilai-b dengan metode maximum likelihood. *Jurnal Sains dan Pendidikan Fisika*, *8*(3), 269–277. https://doi.org/10.35580/jspf.v8i3.927

Pertiwi, I. I. (2022). Analisis statistik distribusi kejadian gempabumi di Luwu Timur, Morowali, dan Morowali Utara, Sulawesi. *Jurnal Geofisika*, *20*(1), 1–7. https://doi.org/10.36435/jgf.v20i1.477

Pertiwi, I. I., & Marniati. (2023). *Kajian seismotektonik di perairan Buton Selatan, Sulawesi Tenggara*. ResearchGate. https://www.researchgate.net/publication/372548857

Pertiwi, I. I., & Marniati. (2024). *Kerapatan sebaran sensor seismik mampu mencatat gempabumi berskala kecil (magnitudo M<2) di wilayah Sulawesi Tenggara dan Sulawesi Selatan*. ResearchGate. https://www.researchgate.net/publication/377846261

Pertiwi, I. I. (2025, January 6). *Tahun 2024, BMKG petakan enam zona aktif gempabumi di wilayah Sulawesi Tenggara*. Antara News Sultra. https://sultra.antaranews.com/berita/489110/

Petersen, M. D., Mueller, C. S., Frankel, A. D., & Zeng, Y. (2008). *Spatial seismicity rates and maximum magnitudes for background earthquakes* (Appendix J). In *The Uniform California Earthquake Rupture Forecast, version 2 (UCERF 2)* (USGS Open-File Report No. 2007-1437J; CGS Special Report No. 203J). U.S. Geological Survey; California Geological Survey.

Purba, J., Priadi, R., Frando, M., & Pertiwi, I. I. (2025). The Purpri fault: A newly identified active fault in East Kolaka, Indonesia, based on HypoDD and DInSAR. *Geološki Anali Balkanskoga Poluostrva*, *86*(1). https://doi.org/10.2298/GABP250417005P

Pusat Studi Gempa Nasional (PuSGeN). (2017). *Peta sumber dan bahaya gempa Indonesia tahun 2017*. Pusat Penelitian dan Pengembangan Perumahan dan Permukiman, Badan Penelitian dan Pengembangan, Kementerian Pekerjaan Umum dan Perumahan Rakyat.

Pusat Studi Gempa Nasional (PuSGeN). (2024). *Peta patahan aktif Indonesia: Sulawesi*. Kementerian Pekerjaan Umum dan Perumahan Rakyat.

Badan Penanggulangan Bencana Daerah (BPBD) Kabupaten Kolaka Timur. (2025). *Laporan kejadian gempabumi tektonik di wilayah Kabupaten Kolaka Timur, Provinsi Sulawesi Tenggara periode 24 Januari–13 Februari 2025* [Report].

Scholz, C. H. (2015). On the stress dependence of the earthquake b value. *Geophysical Research Letters*, *42*(5), 1399–1402. https://doi.org/10.1002/2014GL062863

Shi, H., Meng, L., Zhang, X., Chang, Y., Yang, Z., Xie, W., Hattori, K., & Han, P. (2018). Decrease in b value prior to the Wenchuan earthquake (Ms8.0). *Chinese Journal of Geophysics*, *61*, 1874–1882.

Spada, M., Tormann, T., Wiemer, S., & Enescu, B. (2013). Generic dependence of the frequency-size distribution of earthquakes on depth and its relation to the strength profile of the crust. *Geophysical Research Letters*, *40*, 709–714.

Utsu, T. (1965). A method for determining the value of "b" in a formula log n = a-bM showing the magnitude-frequency relation for earthquakes. *Geophysical Bulletin*, *13*, 99–103.

van der Elst, N. J. (2021). b-positive: A robust estimator of aftershock magnitude distribution in transiently incomplete catalogs. *Journal of Geophysical Research*, *126*(2), Article e2020JB021027. https://doi.org/10.1029/2020JB021027

Wang, R., Chang, Y., Miao, M., Zeng, Z., Chen, H., Shi, H., Li, D., Liu, L., Su, Y., & Han, P. (2021). Assessing earthquake forecast performance based on b value in Yunnan Province, China. *Entropy*, *23*(6), Article 730.

Watkinson, I. M., & Hall, R. (2017). Fault systems of the eastern Indonesian triple junction: Evaluation of Quaternary activity and implications for seismic hazards. In P. R. Cummins & I. Meilano (Eds.), *Geohazards in Indonesia: Earth science for disaster risk reduction* (Geological Society, London, Special Publications, Vol. 441, pp. 71–120). Geological Society of London. https://doi.org/10.1144/SP441.8

Wells, D. L., & Coppersmith, K. J. (1994). New empirical relationships among magnitude, rupture length, rupture width, rupture area, and surface displacement. *Bulletin of the Seismological Society of America*, *84*(4), 974–1002. https://doi.org/10.1785/BSSA0840040974

Wiemer, S., & Wyss, M. (1997). Mapping the frequency-magnitude distribution in asperities: An improved technique to calculate recurrence times? *Journal of Geophysical Research*, *102*(B7), 15115–15128. https://doi.org/10.1029/97JB00726

Wiemer, S., & Wyss, M. (2000). Minimum magnitude of completeness in earthquake catalogs: Examples from Alaska, the western United States, and Japan. *Bulletin of the Seismological Society of America*, *90*(4), 859–869. https://doi.org/10.1785/0119990114

Wiemer, S. (2001). A software package to analyze seismicity: ZMAP. *Seismological Research Letters*, *72*(3), 373–382. https://doi.org/10.1785/gssrl.72.3.373

Wijayanto, Fatchurochman, I., Pranata, B., Gunawan, I., Supendi, P., Daryono, Riama, N. F., & Karnawati, D. (2025). Analisis rangkaian gempabumi Kolaka, Sulawesi Tenggara, tanggal 3–29 Januari 2025. *Artikel BMKG*. https://www.bmkg.go.id/artikel/

Wu, Y. M., Chen, S. K., Huang, T. C., Huang, H. H., Chao, W. A., & Koulakov, I. (2018). Relationship between earthquake b-values and crustal stresses in a young orogenic belt. *Geophysical Research Letters*, *45*, 1832–1837.

Zhang, Y., Wang, R., Shi, H., Miao, M., Zhuang, J., Chang, Y., Jiang, C., Meng, L., Li, D., Liu, L., Su, Y., Zhang, Z., & Han, P. (2025). Earthquake forecasting based on b-value and background seismicity rate in Yunnan Province, China. *Entropy*, *27*(3), Article 205. https://doi.org/10.3390/e27020205